

DETECTION, CHARACTERIZATION AND BIOLOGICAL ACTIVITIES OF [BISPHOSPHO-THR^{3,9}]ODN, AN ENDOGENOUS MOLECULAR FORM OF ODN RELEASED BY ASTROCYTES

K. GACH,^{a,b} O. BELKACEMI,^a B. LEFRANC,^c
P. PERLIKOWSKI,^d J. MASSON,^e M.-L. WALET-BALIEU,^e
J.-C. DO-REGO,^f L. GALAS,^c D. SCHAPMAN,^c
R. LAMTAHRI,^a M.-C. TONON,^a D. VAUDRY,^{a,c,e}
J. CHUQUET^{a†} AND J. LEPRINCE^{a,c,*†}

^aINSERM U982, Laboratory of Neuronal and Neuroendocrine Differentiation and Communication, Neurotrophic Factors and Neuronal Differentiation Team, Institute for Research and Innovation in Biomedicine (IRIB), University of Rouen, Mont-Saint-Aignan, France

^bDepartment of Biomolecular Chemistry, Medical University of Lodz, Lodz, Poland

^cCell Imaging Platform of Normandy PRIMACEN, IRIB, University of Rouen, Mont-Saint-Aignan, France

^dDivision of Dynamics, Technical University of Lodz, Lodz, Poland

^ePlatform of Proteomics PISSARO, IRIB, University of Rouen, Mont-Saint-Aignan, France

^fPlatform of Behavioral Analysis SCAC, IRIB, University of Rouen, Rouen, France

Abstract—Astrocytes synthesize and release endozepines, a family of regulatory neuropeptides, including diazepam-binding inhibitor (DBI) and its processing fragments such as the octadecaneuropeptide (ODN). At the molecular level, ODN interacts with two types of receptors, *i.e.* it acts as an inverse agonist of the central-type benzodiazepine receptor (CBR), and as an agonist of a G protein-coupled receptor (GPCR). ODN exerts a wide range of biological effects mediated through these two receptors and, in particular, it regulates astrocyte activity through an autocrine/paracrine mechanism involving the metabotropic receptor. More recently, it has been shown that Müller glial cells secrete phosphorylated DBI and that bisphosphorylated ODN ([bisphospho-Thr^{3,9}]ODN, bpODN) has a stronger affinity

for CBR than ODN. The aim of the present study was thus to investigate whether bpODN is released by mouse cortical astrocytes and to compare its potency to ODN. Using a radioimmunoassay and mass spectrometry analysis we have shown that bpODN as well as ODN were released in cultured astrocyte supernatants. Both bpODN and ODN increased astrocyte calcium event frequency but in a very different range of concentration. Indeed, ODN stimulatory effect decreased at concentrations over 10⁻¹⁰ M whereas bpODN increased the calcium event frequency at similar doses. *In vivo* effects of bpODN and ODN were analyzed in two behavioral paradigms involving either the metabotropic receptor (anorexia) or the CBR (anxiety). As previously described, ODN (100 ng, icv) induced a significant reduction of food intake. Similar effect was achieved with bpODN but at a 10 times higher dose (1000 ng, icv). Similarly, and contrasting with our hypothesis, bpODN was also 10 times less potent than ODN to induce anxiety-related behavior in the elevated zero maze test. Thus, the present data do not support that phosphorylation of ODN is involved in receptor selectivity but indicate that it rather weakens ODN activity. © 2015 IBRO. Published by Elsevier Ltd. All rights reserved.

Key words: endozepines, diazepam-binding inhibitor, octadecaneuropeptide, phosphorylated peptide, food intake, anxiety.

INTRODUCTION

The octadecaneuropeptide (ODN) belongs to endozepines, a family of regulatory neuropeptides, initially isolated from rat brain and characterized as the endogenous ligands of benzodiazepine receptors (Guidotti et al., 1983). All endozepines described so far derive from an 86-amino acid polypeptide called diazepam-binding inhibitor (DBI) (Guidotti et al., 1983; Tonon et al., 2013). Proteolytic cleavage of DBI generates several biologically active peptides including ODN (DBI_[33–50]) (Ferrero et al., 1986) and the triakontatetra-neuropeptide (TTN) (DBI_[17–50]) (Slobodyansky et al., 1989). The mechanism of action of endozepines is still poorly understood but at the molecular level, ODN would interact with two types of receptors. It acts as an inverse agonist of central-type benzodiazepine receptors (CBR) that are intrinsic components of the GABA_A receptor-chloride channel complex (Ferrero et al., 1984) and as an agonist of a G protein-coupled receptor (GPCR) (Patte et al., 1995; Gandolfo et al.,

*Correspondence to: J. Leprince, INSERM U982, Laboratory of Neuronal and Neuroendocrine Differentiation and Communication, Neurotrophic Factors and Neuronal Differentiation Team, Institute for Research and Innovation in Biomedicine (IRIB), University of Rouen, Mont-Saint-Aignan, France. Tel: +33-235-14-6647.

E-mail address: jerome.leprince@univ-rouen.fr (J. Leprince).

† These authors contributed equally to this work.

Abbreviations: bpODN, [bisphospho-Thr^{3,9}]ODN; CBR, central-type benzodiazepine receptor; CSF, cerebrospinal fluid; DBI, diazepam-binding inhibitor; DIEA, N,N-diisopropylethylamine; DMEM, Dulbecco's modified Eagle's medium; EDTA, ethylenediaminetetraacetic acid; FA, formic acid; FBS, fetal bovine serum; FWHM, full-width half-maximum; GFAP, glial fibrillary acidic protein; GPCR, G protein-coupled receptor; HBSS, Hank's Balanced Salt Solution; HEPES, N-2-hydroxyethyl-piperazine-N-2-ethane sulfonic acid; HOBt, 1-hydroxybenzotriazole; NMP, N-methylpyrrolidone; ODN, octadecaneuropeptide; PLC, phospholipase C; RIA, radioimmunoassay; TBME, tertbutyl-methylether; TBTU, O-benzotriazol-1-yl-N,N,N',N'-tetramethyluronium tetrafluoroborate; TFA, trifluoroacetic acid; TIS, triisopropylsilane.

1997). Indeed, electrophysiological studies show that DBI and ODN attenuate GABA-induced Cl^- efflux in neurons and endocrine cells (Bormann, 1991; Louiset et al., 1993; Alfonso et al., 2012), indicating that endozepines act as negative allosteric modulators of the GABA_A receptors. In parallel, it has been shown that, in cultured rat astrocytes, ODN activates a GPCR, positively coupled either to phospholipase C (PLC) (Patte et al., 1995; Gandolfo et al., 1997; Leprince et al., 2001) or to adenylyl cyclase (Hamdi et al., 2012). From a functional point of view, ODN stimulates neurosteroid biosynthesis (Do Rego et al., 2001) and glial cell or neuroblast proliferation (Gandolfo et al., 1999; Alfonso et al., 2012) through CBR activation, but increases intracellular calcium concentration ($[\text{Ca}^{2+}]_i$) in astrocytes (Gandolfo et al., 1997; Leprince et al., 1998, 2001) and hypothalamic neuropeptide expressions in neurons (Compère et al., 2003, 2004, 2005) through the ODN–GPCR activation. *In vivo*, ODN exerts multiple biological effects. Behavioral studies have demonstrated that ODN, acting through CBR, increases in rodent aggressiveness (Kavaliere and Hirst, 1986), induces anxiety and proconflict behavior (De Mateos-Verchère et al., 1998) but reduces pentobarbital-induced sleeping time (Dong et al., 1999), drinking (Manabe et al., 2001) and pentylenetetrazol-evoked convulsions (De Mateos-Verchère et al., 1999). In addition, ODN acting through its metabotropic receptor exerts a potent anorexigenic effect (De Mateos-Verchère et al., 2001; Do Rego et al., 2007) and relays brain glucose sensing (Lanfray et al., 2013).

Endozepines are widely distributed in the central nervous system (CNS) and peripheral tissues (for review Tonon et al., 2013). In the mammalian brain, endozepines are exclusively synthesized by glial cells. Within the brain, the highest level of DBI-like immunoreactivity has been reported in astroglial cells of the cerebral cortex (Tonon et al., 1990), ependymocytes bordering the third ventricle (Tonon et al., 1990; Malagon et al., 1993; Do Rego et al., 2001), tanycytes of the median eminence (Tonon et al., 1990; Malagon et al., 1993) and Bergmann cells of the cerebellum (Tonon et al., 1990; Vidnyánszky et al., 1994; Yanase et al., 2002). In the retina, DBI is expressed and released by radially oriented Müller glial cells and by stellate astrocytes (Holländer et al., 1991; Barmack et al., 2004; Qian et al., 2008). Moreover, it has been shown that retinal Müller glial cells also secrete a multiphosphorylated form of DBI (Qian et al., 2008). Indeed, four phosphorylation sites were identified in position Ser^2 , Thr^{36} , Thr^{42} and Thr^{65} that fit a protein kinase C and/or a casein kinase II phosphorylation pattern. Interestingly, Thr^{36} and Thr^{42} residues of DBI are located in the sequence of ODN (Thr^3 and Thr^9 residues, respectively). The functional consequence of this post-translational modification is still unclear but it has been reported that phosphorylation of DBI increases its affinity for the GABA_A receptor (Qian et al., 2008). Similarly, threonine-phosphorylated ODN, [bisphospho- $\text{Thr}^{3,9}$]ODN (bpODN), has a higher affinity for the GABA_A receptor than unphosphorylated ODN (Qian et al., 2008).

It is well established that cultured rat astrocytes contain and release DBI-related peptides, including ODN (Lamacz et al., 1996). There is now evidence that ODN acts as both an autocrine factor regulating glial cell activity and a gliotransmitter modulating neurotransmission (Hamdi et al., 2011; Lanfray et al., 2013). However, little is known regarding a possible selectivity of ODN toward the CBR or metabotropic receptors. The aim of the present study was thus to investigate whether bpODN is released by mouse astrocytes, affects their calcium mobilizing dynamics, and exerts different *in vivo* effects than unphosphorylated ODN.

EXPERIMENTAL PROCEDURES

Reagents

All Fmoc-amino-acid residues, O-benzotriazol-1-yl-N,N,N',N'-tetramethyluronium tetrafluoroborate (TBTU), and 1-hydroxybenzotriazole (HOBt) were purchased from PolyPeptide (Strasbourg, France), Novabiochem Merck Chemicals (Nottingham, UK) or Christof Senn Laboratories (Dielsdorf, Switzerland). Preloaded 4-hydroxymethyl-phenoxyethyl-copolystyrene-1%-divinylbenzene resin (Fmoc-Lys(Boc)-HMP) was from Life Technologies (Villebon sur Yvette, France). N,N-Diisopropylethylamine (DIEA), piperidine, trifluoroacetic acid (TFA), and triisopropylsilane (TIS) were supplied from Acros Organics (Geel, Belgium). N-Methylpyrrolidone (NMP), dichloromethane (DCM), chloramine-T, Triton X-100, γ -globulins from bovine blood, fetal bovine serum (FBS), and other reagents were purchased from Sigma–Aldrich (Saint-Quentin-Fallavier, France). Dulbecco's modified Eagle's medium (DMEM), F12 culture medium, L-glutamine, HEPES, trypsin-ethylenediaminetetraacetic acid (trypsin–EDTA), antibiotic–antimycotic solution and Hank's Balanced Salt Solution (HBSS) were supplied from Gibco (Invitrogen, Grand Island, NY, USA). Fluo-4 AM was obtained from Molecular Probes (Invitrogen, Grand Island, NY, USA). Na^{125}I (2000 Ci/mmol) was from Amersham International (Les Ulis, France). Acetonitrile was purchased from Fisher Scientific (Illkirch, France).

Peptide synthesis

Mouse/rat ODN (H-Gln-Ala-Thr-Val-Gly-Asp-Val-Asn-Thr-Arg-Pro-Gly-Leu-Leu-Asp-Leu-Lys-OH) and its C-terminal octapeptide OP (H-Arg-Pro-Gly-Leu-Leu-Asp-Leu-Lys-OH) were synthesized as previously described (Leprince et al., 1998, 2001). Phosphothreonine-containing peptides, bpODN (H-Gln-Ala-Thr($\text{PO}(\text{OH})_2$)-Val-Gly-Asp-Val-Asn-Thr($\text{PO}(\text{OH})_2$)-Asp-Arg-Pro-Gly-Leu-Leu-Asp-Leu-Lys-OH), [Cys⁰]bpODN (H-Cys-Gln-Ala-Thr($\text{PO}(\text{OH})_2$)-Val-Gly-Asp-Val-Asn-Thr($\text{PO}(\text{OH})_2$)-Asp-Arg-Pro-Gly-Leu-Leu-Asp-Leu-Lys-OH) and [Tyr⁰]bpODN (H-Tyr-Gln-Ala-Thr($\text{PO}(\text{OH})_2$)-Val-Gly-Asp-Val-Asn-Thr($\text{PO}(\text{OH})_2$)-Asp-Arg-Pro-Gly-Leu-Leu-Asp-Leu-Lys-OH) were synthesized (0.1-mmol scale) by the solid phase methodology on a Fmoc-Lys(Boc)-HMP resin using a 433A Applied Biosystems peptide synthesizer (AB Sciex, Courtaboeuf, France) and the standard Fmoc manufacturer's

procedure. All Fmoc-amino-acids (1 mmol, 10 eq.) were coupled by *in situ* activation with TBTU/HOBt (1.25 mmol:1.25 mmol, 12.5 eq.) and DIEA (2.5 mmol, 25 eq.) in NMP. Peptides were deprotected and cleaved from the resin by adding 10 ml of the mixture TFA/TIS/H₂O (99.5:0.25:0.25, v/v/v) for 120 min at room temperature. After filtration, crude peptides were precipitated by the addition of tertbutylmethylether (TBME), centrifuged (4500 rpm), washed twice with TBME, and freeze-dried. The synthetic peptides were purified by reversed-phase HPLC on a 2.2 × 25-cm Vydac 218TP1022 C₁₈ column (Grace, Epernon, France) by using a linear gradient (10–50% over 45 min) of acetonitrile/TFA (99.9:0.1; v/v) at a flow rate of 10 ml/min. Analytical HPLC, performed on a 0.46 × 25-cm Vydac 218TP54 C₁₈ column (Grace), showed that the purity of all peptides was >99.9% (Table 1). The purified peptides were characterized by MALDI-TOF mass spectrometry on a Voyager DE PRO (AB Sciex) in the reflector mode with α -cyano-4-hydroxycinnamic acid as a matrix and peptides of known molecular mass as calibrates.

Animals

All experiments were conducted by authorized investigators in accordance with the European Communities Council Directive of 24 November 1986 (86/609/EEC), and approved by the Local Ethics Committee for Animal Research (N/02-02-12/05/02-15). Male Swiss albino CD1 mice (IFFA-CREDO/Charles River, Saint-Germain sur l'Arbresle, France), weighing 22–25 g, were used for *in vivo* experiments. Animals were housed with free access to standard laboratory diet (U.A.R., Villemoisson-sur-Orge, France) and tap water, under controlled temperature (22 ± 1 °C) and lighting (light from 7:00 a.m. to 7:00 p.m.). Newborn (24–48 h) C57BL/6 mice (IFFA-CREDO/Charles River) were used to prepare secondary cultures of mouse cortical astrocytes for *in vitro* experiments. New Zealand rabbits (IFFA-CREDO/Charles River) weighing 2–4 kg were used to raise bpODN antisera.

Immunization

Polyclonal antibodies against bpODN were raised in rabbits as previously described (Servili et al., 2011). The immunogen was prepared by conjugating [Cys⁰]bpODN (4 mg, RP-HPLC purity >99%) to 5.5 mg maleimide-activated

keyhole limpet hemocyanin (MilleGen, Labège, France). Two New-Zealand rabbits were injected intradermally at multiple sites with an equivalent of 200 μ g of hapten (reconstituted in 1 ml phosphate-buffered saline, PBS) emulsified with 1 ml complete Freund's adjuvant for the first injection and 1 ml incomplete Freund's adjuvant for subsequent injections (Sigma–Aldrich). Injections were repeated at monthly intervals, and blood samples were collected 1 week after the third and subsequent immunizations. Antisera were stored at –80 °C until use.

Cell culture

Secondary cultures of mouse cortical astrocytes were prepared as previously described (Masmoudi et al., 2005) with minor modifications. Briefly, cerebral hemispheres from newborn C57BL/6 mouse were collected in DMEM/F12 (2:1; v/v) culture medium supplemented with 2 mM L-glutamine, 1‰ insulin, 5 mM HEPES, and 1% of the antibiotic–antimycotic solution. The tissues were dissociated mechanically with a syringe equipped with a 1-mm gauge needle, and filtered through a 100- μ m sieve (Falcon, Franklin Lakes, NJ, USA). Dissociated cells were resuspended in culture medium supplemented with 10% FBS, plated in 75-cm² flasks (Greiner Bio-one GmbH, Frickenhausen, Germany) and incubated at 37 °C in a 5% CO₂/95% O₂ atmosphere. When cultures were confluent, astrocytes were isolated by shaking overnight the flasks on an orbital agitator. Adhesive cells were detached by trypsinization and seeded for 5 min to discard contaminating microglial cells. Then, the non-adhering astrocytes were harvested and plated in 75-cm² flasks at the density of 1 × 10⁵ cells/ml for endozepine release determination or in glass-bottomed dishes (P35G-1.0-20-C, MatTek Corporation, Ashland, MA, USA) at the density of 1.75 × 10⁵ cells/ml for calcium imaging experiments. All experiments were performed on 48- to 72-h-old secondary cultures (80% confluence). In these conditions, more than 97% of the cells were labeled with antibodies raised against glial fibrillary acidic protein (GFAP) (Fig. 3).

BpODN radioimmunoassay (RIA)

To characterize bpODN in culture media of secondary cultured mouse cortical astrocytes a RIA was implemented combined with mass spectrometry analysis. The culture medium was removed and cells were rinsed twice with FBS-free medium and then

Table 1. Chemical data for compounds

Peptide	RP-HPLC		MS	
	RT (min) ^a	Purity (%)	Cacl _d (amu) ^b	Obsd (amu) ^c
ODN	18.06	99.9	1911.01	1911.89
OP	17.62	99.9	910.56	911.45
bpODN	25.47	99.8	2070.94	2071.67
[Cys ⁰]bpODN	21.83	99.9	2173.95	2175.28
[Tyr ⁰]bpODN	24.27	99.9	2234.00	2234.98

^a Retention time determined by reversed-phase HPLC.

^b Theoretical monoisotopic molecular weight (calculated).

^c MH⁺ value assessed by MALDI-TOF-MS (observed). RT, retention time. Amu, atomic mass unit.

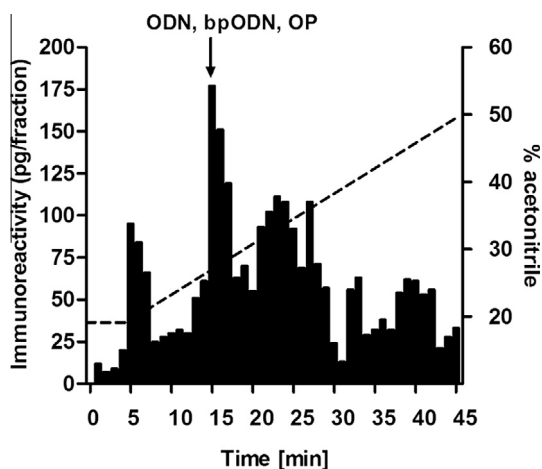


Fig. 1. Reversed-phase HPLC analysis of the supernatant content collected from secondary cultures of mouse cortical astrocytes. All fractions collected (1 ml each) were dried and assayed for bpODN-like immunoreactivity (bpODN-LI) using RIA. The arrow indicates the co-elution position of synthetic rat ODN, bpODN and OP. The dashed line represents the concentration of acetonitrile in the eluting solvent.

incubated for 1 h in the same medium at 37 °C in a humid atmosphere containing 5% CO₂. Astrocyte-conditioned media from three culture 75 cm² flasks (~3 × 10⁷ cells/dish) were collected and then centrifuged at 11,000g for 10 min. The supernatants were desalted and preconcentrated using a Sep-Pak C₁₈ cartridge (Waters Corp., Milford, MA, USA). Bound material was eluted with 50% (v/v) acetonitrile/water containing 0.1% TFA (v/v), the solvent was evaporated by vacuum centrifugation (Speed Vac concentrator, Savant, Hicksville, NY, USA). Dried samples of cultured medium were reconstituted in 10% (v/v) acetonitrile/water containing 0.1% TFA (v/v) and analyzed by reversed-phase HPLC on a Phenomenex C₁₈ column (0.45 × 25 cm) (Phenomenex, Torrance, CA, USA) by using a linear gradient (20–50% over 40 min) of acetonitrile/TFA (99.9:0.1, v/v) at a flow rate of 1 ml/min. One-ml fractions were collected and evaporated by vacuum centrifugation. bpODN-like immunoreactivity (bpODN-LI) was measured in each fraction by RIA, as previously described (Tonon et al., 1990) using the antiserum against synthetic rat bpODN. Briefly, concentrated sample of each HPLC fraction was reconstituted in phosphate buffer (100 mM; pH 8) containing 0.1% Triton X-100. Synthetic rat [Tyr⁰]bpODN (1 μg) was radiolabeled with 0.5 mCi of Na¹²⁵I using the chloramine-T procedure, as previously described (Vaudry et al., 1978). Monoiodinated [¹²⁵I-Tyr⁰]bpODN, labeled on the Tyr⁰ residue, was purified by reversed-phase HPLC on a 0.46 × 25-cm Adsorbosphere C₁₈ column (Grace) by using a linear gradient (10–40% over 40 min) of acetonitrile/TFA (99.9:0.1, v/v) at a flow rate of 1 ml/min. Monoiodinated [¹²⁵I-Tyr⁰]bpODN eluted at 28% acetonitrile. After a 2-day incubation at 4 °C with bpODN antiserum (final dilution 1:40,000) and the tracer, the antibody-bound bpODN fraction was precipitated by the addition of 100 μl bovine γ-globulins (1%, w/v) and 2 ml polyethylene

glycol (20%, w/v). After centrifugation (5000g, 4 °C, 30 min), the supernatant was removed and the pellet containing the bound fraction was counted in a gamma counter (LKB Wallac, Mt. Waverley, Australia). The total amount of tracer was 6000 cpm/tube. The working range of the RIA was 5–2500-pg/tube.

Mass spectrometry characterization

HPLC fraction (1 ml) corresponding to the highest immunoreactive fraction was evaporated by vacuum centrifugation and dissolved in 20 μl of acetonitrile/water (97:3, v/v) containing 0.1% formic acid (FA) (v/v). The fraction was submitted on a NanoLC-ChipCube system equipped with a Chip 150-mm Zorbax 300SB-C18, 5-μm particles size, high capacity 4 μg “on column”, coupled to a 6340 ion trap mass spectrometer (Agilent Technologies, Les Ulis, France). After a pre-concentration step, peptides were eluted from the analytical column (150-mm × 75-μm, volume 600 nl) by using a linear gradient (3–45% over 20 min) of acetonitrile/water/FA (89.95:9.95:0.1, v/v/v) at a flow rate of 0.45 μl/min. The ESI(+)-ion trap mass spectrometer was operated using 6300 series TrapControl software 6.1 (Bruker Daltonik). Optimized ionization parameters used were as follows: capillary voltage, 1885 V; drying gas flow rate, 5 l/min; drying temperature, 300 °C. Trap MS data acquisition was performed in the full-scan MS mode at the mass range of *m/z* 300–2000 including mass of 456.8, 638.2, 948.1 and 691.7. Data were analyzed using Data Analysis software 3.4 (Bruker Daltonik). Synthetic ODN (*m/z* (+3) = 638.2), bpODN (*m/z* (+3) = 691.7) and OP (*m/z* (+2) = 456.8) were analyzed at the concentration of 200 pg/μl to determine the retention time and *m/z* value of these three standards.

Calcium imaging

After 48–72 h of culture on glass bottom dishes, cells were incubated with 3 μM of Fluo-4-AM diluted in HBSS (pH = 7.4) at 37 °C for 30 min in the dark. Thereafter, cells were rinsed twice with 2 ml HBSS. The dish was then placed on the stage of an inverted confocal microscope (TCS SP5 II, Leica Microsystems, Wetzlar, Germany) and illuminated at 488 nm through a 20× objective at 37 °C. Images of a field of view including 30–60 cells were recorded as a time series (512 × 512 pixels at the frequency of 1 Hz over 20 min including a 10-min control period (0–10 min) and a 10-min treatment period (10–20 min). Peptides, dissolved in HBSS, were gently infused using a pipette (100 μl over 5 s). In the same infusion conditions, no measurable effect on calcium transients was recorded with HBSS alone (Fig. 4).

Image analysis

Image sequences were analyzed with a semi-automatic detection and measurement algorithm written in MATLAB (MathWorks, Inc., Natick, MA, USA). All traces were smoothed with moving-average filter (window size

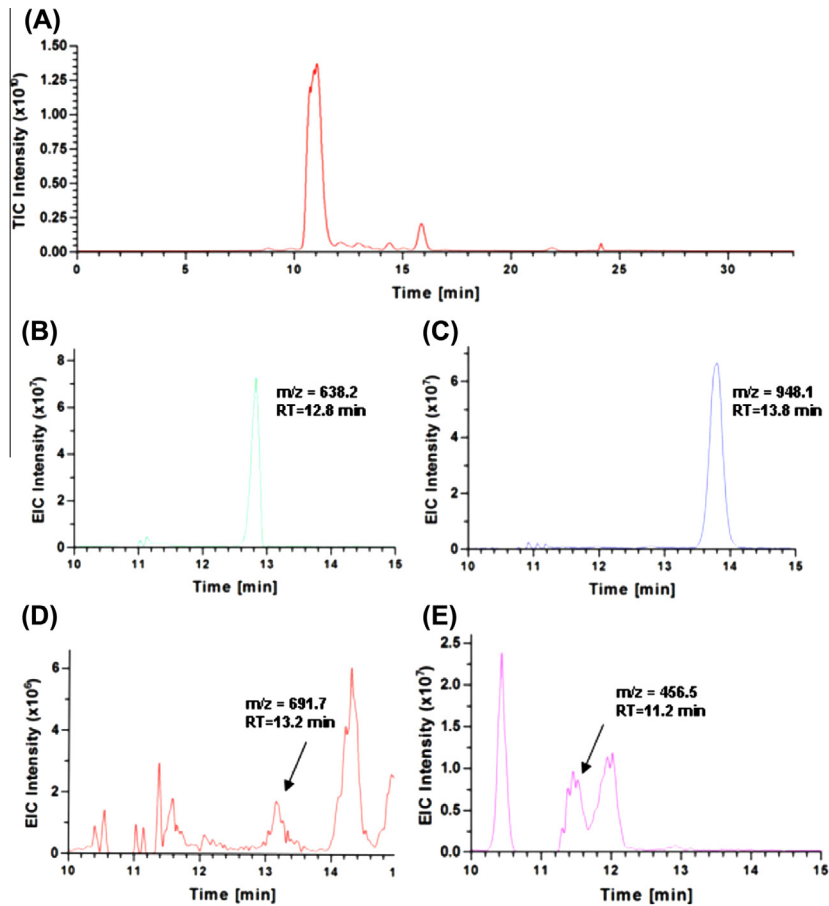


Fig. 2. Total ion current (TIC) chromatogram (A) and extracted-ion chromatograms (EIC) of ODN (B), [pGlu¹]ODN (C), bpODN (D) and OP (E). RT, retention time.

of five frames) before the detection procedure. Briefly, $[Ca^{2+}]_i$ changes were quantified by measuring the mean pixel value of manually selected somatic area in each cell of each frame of the image stack. Signals were expressed as relative fluorescence changes ($\Delta F/F_0$), where F_0 was the mean of the lowest 20% of the somatic fluorescence signals over a 10-min baseline period. $[Ca^{2+}]_i$ peaks were automatically detected according to a threshold set for each peak by the operator who thereafter checked all detected Ca^{2+} events. Event duration was defined as the time-interval between the point when the peak reached 50% of maximal amplitude and the point when it declined back to 50% (full-width half-maximum, FWHM). Rise time was defined as the time required for the peak to increase from 0% to 100% of its maximal amplitude.

Susceptibility of peptides to degradation in cerebrospinal fluid (CSF)

Time-course stability of bpODN and ODN in CSF was assessed *in vitro* by mass spectrometry according to a procedure adapted from Neveu et al. (2012). Briefly, 45 μ l of bpODN (27 μ g) or ODN (42 ng) was incubated at 37 °C with 45 μ l fresh rat CSF in triplicate. The reaction was stopped after different times (0, 5, 15, 35, 60, 120 and 240 min) by adding, to 10 μ l samples in triplicate, 10 μ l TFA (30% in water). Each replicate was

freeze-dried and stored at -18 °C until analyzed. Aliquots were rehydrated in 120 μ l of H₂O/TFA (99.9:0.1) and the peptide content pre-purified on ZipTips C₁₈ (Agilent Technologies) with 500 μ l acetonitrile/H₂O/TFA (59.95:39.95:0.1). Eluting solvent was evaporated by vacuum centrifugation and the peptidic material was dissolved in 10 μ l acetonitrile/H₂O (3:97) containing 0.1% FA. Samples (1 μ l) were analyzed in triplicate on an UPLC system coupled to a 6490 ESI(+)-triple quad mass spectrometer (Agilent Technologies). Peptides were eluted from an Acquity CSH C₁₈ column (100 \times 2.1 mm, 1.7 μ m) using a linear gradient (3–40% over 5 min) of acetonitrile/H₂O/FA (89.95:9.95:0.1) at a flow rate of 0.4 μ l/min. Optimized ionization parameters used were as follows: capillary voltage, 3500 V; drying gas flow rate, 14 l/min; drying temperature, 250 °C. MS data acquisition was performed in the MRM mode with the following majority transitions: ODN (638.01–756.90) and bpODN (691.32–796.89). Data were analyzed using MassHunter Quantitative Analysis software B.06 (Agilent Technologies). ODN and bpODN respective transition areas were used to calculate the percentage of intact compound remaining at the various time points during the incubation. Tendency curves were fitted using the software Prism (GraphPad Software, San Diego, CA, USA) from exponential decay and linear functions for ODN and bpODN, respectively.

In vivo experiments

Intracerebroventricular injection. Intracerebroventricular (icv) injections (10 μ l/mouse) were performed in the left ventricle of manually immobilized mice, within about 3 s, according to the procedure of [Haley and McCormick \(1957\)](#), using an Hamilton microsyringe (50 μ l; Hamilton, Bonaduz, Switzerland) connected to a needle (diameter 0.5 mm) equipped with a guard at 3.5 mm from the tip to control its penetration into the brain. ODN (100-ng/animal), bpODN (10-, 100-, 1000-ng/animal) and ODN + bpODN (100-ng + 1000-ng/animal, respectively) were extratemporaneously dissolved in saline (0.9% NaCl).

Food intake measurement. The effect of ODN and bpODN on food intake was assessed in food-deprived mice (fasted mice), as previously described ([Do Rego et al., 2007](#)). Mice were isolated in individual cages 2 days before the experiments with free access to water and food pellets left on the floor of the cages. Eighteen hours before testing (3:00 p.m.–9:00 a.m.), animals were deprived of food and had access to water *ad libitum*. At 9:00 a.m., 10 min after the icv administration, mice had access to a weighed food pellet (5 g) left on the floor of the cage. During the test, every 30 min for 3 h, the pellet was briefly (< 20 s) removed with forceps and weighed.

Elevated zero maze test. The anxiogenic activity of ODN and bpODN was assessed in the elevated zero maze test, based on the natural aversion of mice to elevated and open spaces. The apparatus consisted of an infrared circular black plexiglas platform (outer diameter 45 cm, width 6 cm), placed 60 cm above the ground level in a dimly illuminated room, divided equally into four quadrants. Two opposite quadrants were surrounded by walls (27 cm high; closed quadrants) while the two other quadrants were devoid of enclosing walls (open quadrants). Fifteen min before the experiments, the animals were isolated in small individual cages at a room temperature of 22 ± 1 °C. Ninety minutes after the icv injection of vehicle, or peptide of interest, each animal was placed at the end of the open section, with the head facing a closed quadrant. The number of entries, the time spent and the distance traveled in open and closed quadrants during a 5-min period were recorded using an automated image analysis system (Ethovision v9.0, Noldus Information Technologies, Wageningen, The Netherlands). The animal was considered to be in an open quadrant or closed quadrant when the centroid of its image (recorded by a video camera) cross the threshold of a quadrant.

Statistical analysis

Statistical analyses were performed using Prism 4.0 (GraphPad Software Inc.). Data are expressed as mean \pm SEM. Differences between groups were assessed by a one-way analysis of variance (ANOVA) followed by a post hoc multiple comparison Student–Newman–Keuls test. Student's *t*-test was used to

compare single treatment to control. A probability level of 0.05 or lower was considered as statistically significant.

RESULTS

Detection and characterization of endozepines released from cultured mouse astrocytes

HPLC analysis of supernatant from secondary cultured cortical mouse astrocytes revealed the presence of spontaneously released bpODN-LI compounds with retention times similar to bpODN, ODN and OP ([Fig. 1](#)). To further characterize the molecular forms of endozepines released, mass spectrometry analysis of the highest immunoreactive fraction was used. The total ion current chromatogram showed two major signals in this pre-purified fraction ([Fig. 2A](#)). Extraction ion current revealed the presence of native ODN characterized by its tri-charged ion ($[MH_3]^{3+} = 638.2$; [Fig. 2B](#)), pyroglutamic form of ODN ($[pGlu^1]ODN$) characterized by its di-charged ion ($[MH_2]^{2+} = 948.1$; [Fig. 2C](#)), bpODN characterized by its tri-charged ion ($[MH_3]^{3+} = 691.7$; [Fig. 2D](#)), and OP characterized by its di-charged ion ($[MH_2]^{2+} = 456.5$; [Fig. 2E](#)). Extraction-ion chromatogram intensities for ODN and $[pGlu^1]ODN$ were very similar whereas the intensities of OP and bpODN were 7- and 35-fold less abundant, respectively.

Calcium imaging in cultured mouse astrocytes

To test the functional specificity of bpODN vs ODN, we have used the ability of secondary cultured astrocytes to respond to ODN by a transient elevation of $[Ca^{2+}]_i$. The culture preparation showed a high proportion of astrocytes since $97.0 \pm 0.5\%$ of the cells were immunopositive for GFAP, a specific marker of astrocytes ([Fig. 3](#)). Astrocytes loaded with the fluorescent calcium-sensitive indicator Fluo-4-AM appeared as a single-cell layer homogeneously paved ([Fig. 3](#)). For imaging, we selected a field of 30–60 cells ($100\text{--}200 \mu\text{m}^2$) scanned at the frequency of one image per second. During the baseline period (10-min, 0–10 min), *i.e.* before any treatment, 90.5% of astrocytes exhibited spontaneous activity with an average frequency of 8.8 ± 0.2 mHz while 9.5% of them remained silent (1079 cells from 37 dishes). The following analysis was therefore based only on active astrocytes, defined as cells showing, at least, one calcium event during the 10-min duration of the baseline period. During this control period, spontaneous Ca^{2+} events had a rise time of 22.5 ± 0.2 s, a peak amplitude of $58.9 \pm 0.6\%$ ($\Delta F/F_0$) and a duration (expressed at FWHM) of 15.4 ± 0.1 s. Overall, these features are in agreement with the somatic calcium dynamics of astrocytes observed *in vitro* or *in vivo* ([Parri and Crunelli, 2003](#); [Schipke et al., 2008](#)). After the baseline period of 10 min, ODN (100 μ l over 5 s) was infused into the culture medium at various concentrations (10^{-10} to 10^{-7} M). The infusion by itself did not elicit any perturbation of the system since neither the frequency nor the shape of calcium elevations was changed when the vehicle solution was used ([Fig. 4](#)). Assays with fluorescein

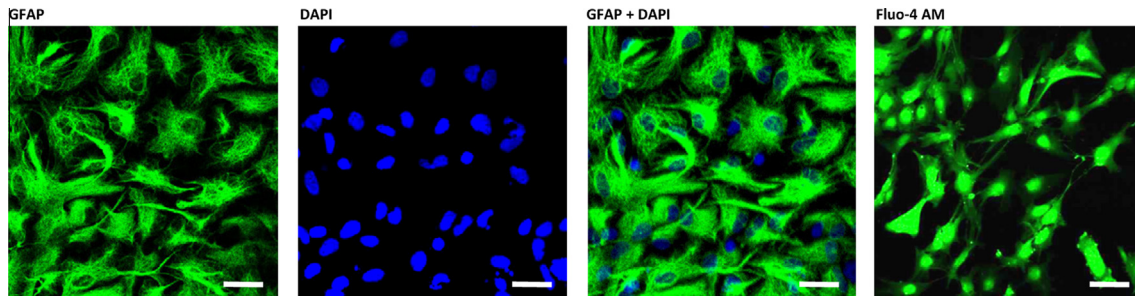


Fig. 3. Homogeneity of cultured astrocytes. Nearly all the cells identified with the DAPI immunostaining were GFAP positive as illustrated by the merge image (GFAP + DAPI). Right: astrocytes loaded with the calcium-sensitive dye Fluo-4-AM. Scale bars = 10 μ m.

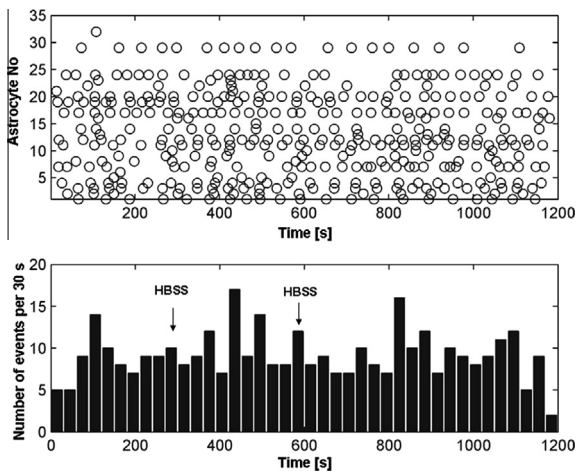


Fig. 4. Effect of infusion of the vehicle solution on astrocytes activity. Upper panel is a raster plot showing the activity of each astrocyte from a representative experiment (31 cells over 20 min) each calcium event being represented by an open dot. Lower panel: total number of calcium event across the trial in time bin of 30 s. The arrows indicate infusion of 100 μ l of the vehicle solution (HBSS).

solution showed that homogenization in the dish was reached after 8 ± 1 s. ODN significantly increased astrocyte calcium activity at the concentration of 10^{-10} M (transient frequency rose by 1.4 ± 0.4 mHz; Fig. 5A, B). At this concentration, ODN also modified the average shape of each single event by increasing the amplitude of Ca^{2+} surges (Table 2). At higher concentrations (10^{-9} to 10^{-8} M), ODN was less active, following a dose-dependent effect on calcium event frequency (Fig. 5A). At 10^{-7} M, ODN slowed the frequency by 1.0 ± 0.5 mHz compared to that of the control period (Fig. 5A, C) and affected all the parameters of the calcium transient shape (Table 2). In contrast, the effect of bpODN on astrocyte calcium activity increased with the dose, starting from an inhibitory effect on calcium event frequency at 10^{-10} M (-0.8 ± 0.3 mHz, Fig. 5D, E) to a stimulatory one at 10^{-7} M (1.4 ± 0.3 mHz, Fig. 5D, F). However at such concentrations of bpODN, calcium transient event shape was similar to the one observed in control conditions (Table 2). Interestingly, the effect of bpODN on calcium event frequency was significant in the two consecutive 5-min periods after the onset of the treatment while ODN effect was only significant in the first 5-min period (Fig. 6).

Effect of bpODN on food consumption in food-deprived mice

To compare the effects of bpODN and ODN on feeding behavior, both compounds were icv injected in food-deprived mice. The anorexigenic effect of ODN is well established and this peptide was used for comparison at the effective dose of 100 ng. BpODN mimicked the effect of ODN, although its efficacy and potency were weaker (Fig. 7A). BpODN reduced the cumulative food consumption in a dose-dependent manner and the strongest effect was observed at the highest injected dose (1000 ng). The dose of 100 ng of bpODN significantly reduced cumulative food intake after 120 min and at the end of 3-h of food presentation. The 120-min cumulative food intake decreased by $26.0 \pm 1.8\%$ and $57.4 \pm 8.5\%$, for a dose of 100 ng of bpODN and ODN, respectively (Fig. 7A). Co-administration of bpODN (1000 ng) and ODN (100 ng) led to a further reduction in food intake albeit lower than the sum of the individual effect (Fig. 7B).

Anxiogenic effect of bpODN in elevated zero-maze test in mice

The putative anxiogenic effect of bpODN was studied in the elevated zero-maze test in mice, 90 min after icv injection of the peptide. The doses of 10 and 100-ng/animal of bpODN and 100-ng/animal of ODN did not significantly reduce the total distance traveled in the maze (Table 3). A significant decrease of the total distance traveled was noticed only at the highest dose of bpODN (1000-ng/animal) reaching $68.9 \pm 9.6\%$ of the control value. A reduction in the number of entries into the open quadrants of the elevated zero-maze was observed for mice injected with a dose of 100 and 1000 ng of bpODN (Table 3). BpODN also induced a dose-dependent reduction and an increase of the time spent in the open and closed quadrants, respectively (Table 3, Fig. 8). However, the effect exerted by the highest dose of bpODN (1000-ng/animal) was weaker than that caused by ODN (100-ng/animal), which strongly decreased the number of entries and the time spent into the open arms (Table 3) and conversely increased the time spent in the closed quadrants of the zero-maze (Fig. 8).

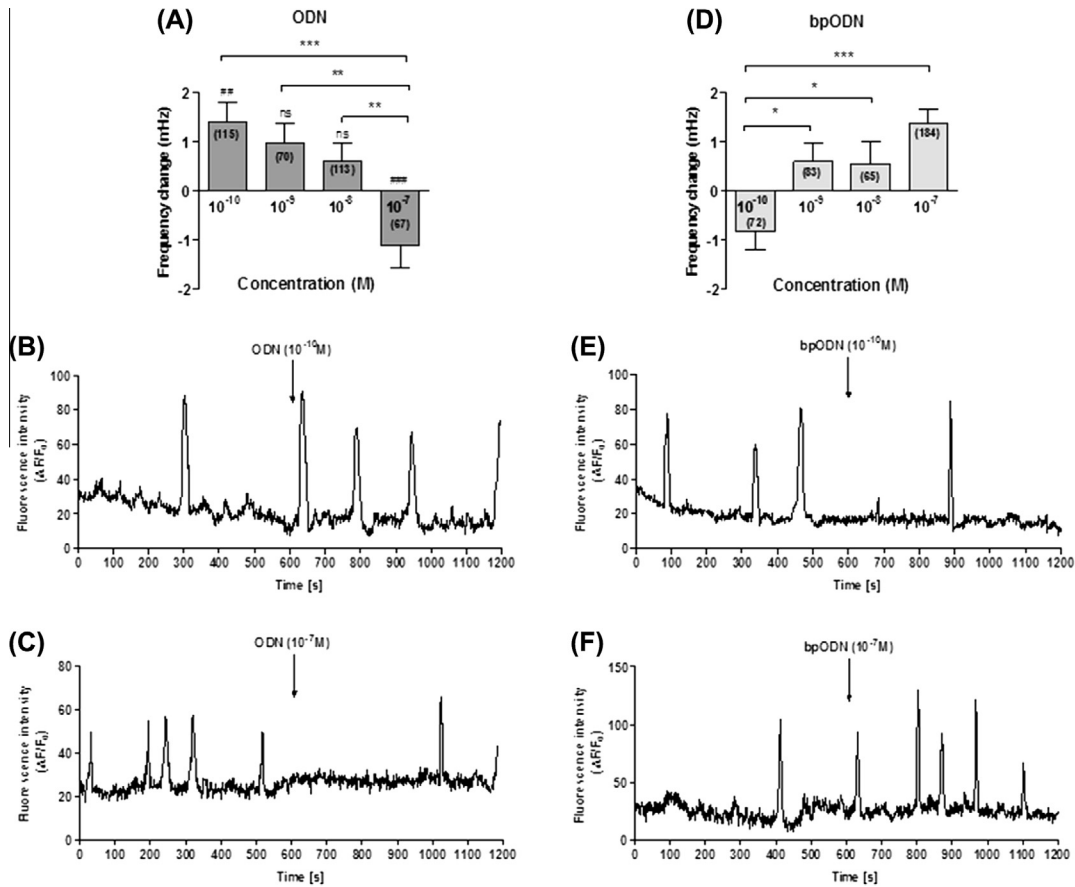


Fig. 5. Effect of graded concentrations of ODN (A) and bpODN (D) on the frequency of spontaneous $[Ca^{2+}]_i$ events in secondary cultures of mouse cortical astrocytes. Each value represents mean \pm SEM of the frequency change calculated from at least 4–5 different dishes from three independent cultures (*i.e.* a negative value reporting a decrease of the frequency relative to the 10-min baseline period). The number of cells studied is indicated in parentheses. Statistical significance was assessed using a one-way ANOVA and a post hoc multiple comparison Student–Newman–Keuls test. * $p < 0.05$, ** $p < 0.01$, *** $p < 0.001$ for comparison of different concentrations of ODN or bpODN. ## $p < 0.01$, ### $p < 0.001$, ns not significantly different for bpODN vs ODN at the same dose. Representative traces of the effect of 10^{-10} M (B) and 10^{-7} M ODN (C), 10^{-10} M (E) and 10^{-7} M (F) bpODN on frequency change of spontaneous $[Ca^{2+}]_i$ oscillations in a single mouse astrocyte.

Table 2. Ca^{2+} event parameters

		<i>n</i>	Amplitude $\Delta F/F_0$ (%)	Duration FWHM (s)	Rise time (s)
bpODN	Control	168	58.3 ± 0.6	20.3 ± 0.9	27.8 ± 1.2
	10^{-10} M	166	58.4 ± 2.6	21.6 ± 0.9	29.2 ± 1.3
	Change		+0.2%	+6.4%	+5.0%
	Control	515	44.1 ± 2.0	18.2 ± 0.4	22.7 ± 0.6
	10^{-7} M	651	47.2 ± 1.7	17.4 ± 0.4	21.6 ± 0.5
	Change		+7.0%	-4.4%	-4.8%
ODN	Control	554	$51.6 \pm 1.8^*$	18.3 ± 0.4	22.7 ± 0.5
	10^{-10} M	679	$57.3 \pm 1.9^*$	17.7 ± 0.4	21.7 ± 0.5
	Change		+11.0%	-3.3%	-4.4%
	Control	541	$68.4 \pm 1.9^*$	14.5 ± 0.3	18.7 ± 0.4
	10^{-7} M	514	$58.7 \pm 1.8^{***}$	$15.8 \pm 0.4^*$	$20.2 \pm 0.5^*$
	Change		-14.2%	+9.0%	-8.0%

Statistical significance was assessed using Student's *t*-test. * $p < 0.05$ and *** $p < 0.001$ vs individual control period. FWHM, full width at half maximum. Change (%) represents the difference between the control and the treatment period.

DISCUSSION

Protein phosphorylation is one of the most prevalent intracellular protein modifications that plays a pivotal

role to regulate various cellular processes including cell proliferation, differentiation, and apoptosis (Pawson and Scott, 1997; Graves and Krebs, 1999; Shumyantseva et al., 2014). It is estimated that 30% of all proteins in a

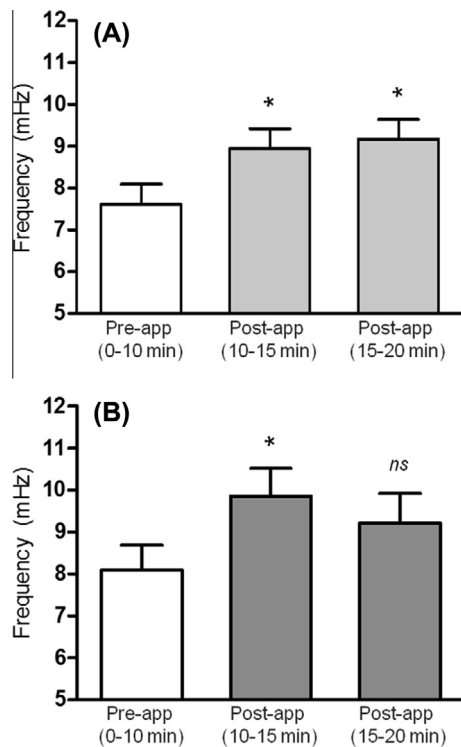


Fig. 6. Reversibility of bpODN- (A) or ODN-mediated (B) calcium changes in astrocytes. bpODN (10^{-7} M) or ODN (10^{-10} M) modified calcium event frequency in the first 5-min period after their single application in cultured astrocytes (10–15-min period, $*p < 0.05$). bpODN effect was still significant in the second 5-min period (15–20 min period, $*p < 0.05$), while ODN effect was no longer significantly different after 5 min (15–20-min period, $p > 0.05$). Statistical significance was assessed using Student's *t*-test. Pre-app: pre-application period; Post-app: post-application period.

cell are phosphorylated at any given time. Phosphorylation of serines and threonines is one of the most widespread post-translational modifications in nature, and probably the most common cellular regulatory mechanism (Hubbard and Cohen, 1993; Hoffmann et al., 1999). A fundamental understanding of these biological processes, at the molecular level, requires characterization of the phosphorylated proteins/peptides.

It is well established that cultured rat astrocytes contain and release substantial amounts of DBI-related peptides, including ODN (Lamacz et al., 1996). By implementing a RIA combined with a mass spectrometry analysis we have shown the occurrence of native ODN and bpODN as well as $[pGlu^1]ODN$ and OP in culture media of secondary cultured mouse cortical astrocytes. To the best of our knowledge, characterization of $[pGlu^1]ODN$, bpODN and OP from cultured astrocyte supernatant has never been reported before. $[pGlu^1]ODN$ may occur as a normal processing of DBI or may be artefactually formed in the culture medium. It has been shown that $[pGlu^1]ODN$ exhibits 61% of the efficacy of ODN to elicit Ca^{2+} response in silent cultured rat astrocytes, suggesting that a free N-terminal amine function is required for full activity of ODN (Leprince et al., 1998). On the other hand, OP, the C-terminal octapeptide of ODN, retains full biological activity (Leprince et al., 1998). Currently, the functional consequence of the bisphosphorylation of ODN is

still unclear. However, it has been shown that this modification is required for optimal binding to CBR (Qian et al., 2008). Hence, understanding the function of this post-translational modification could provide new insights into the mechanism that directs ODN to CBR or metabotropic receptors.

To test the *in vitro* functional specificity of bpODN vs ODN, we have studied the dynamics of intracellular $[Ca^{2+}]_i$ changes in astrocytes using confocal fluorescence microscopy. Intracellular calcium events are the predominant forms of astrocyte signaling activity (Schipke et al., 2008). The spatiotemporal characteristics of these Ca^{2+} changes (frequency, amplitude, duration...) may code for various information of the astrocyte communication within the cellular network (De Bock et al., 2014). The effect of ODN on $[Ca^{2+}]_i$ in single astrocytes has been well documented. ODN increases intracellular calcium concentration in cultured rat astrocytes through activation of a GPCR, which is positively coupled to PLC (Lamacz et al., 1996; Gandolfo et al., 1997). Thus, we have compared the influence of bpODN and ODN on different parameters of calcium dynamics. Both peptides exerted a dose-dependent effect on calcium event frequency. The effect of ODN vanished 5 min after its application while the bpODN effect remained during the 10-min post-treatment period, suggesting that bpODN was more stable than ODN in the presence of cultured astrocytes. In support of this hypothesis, ODN was gradually catabolized *in vitro* by CSF, while bpODN was almost not degraded in the same conditions (Fig. 9). It should be noted that ODN was more stable in CSF than in plasma (data not shown) as generally reported for neuropeptides like Tyr-MIF-1 (Kastin et al., 1994). These data suggest that bpODN would be a stabilized form of ODN which may have different roles. Indeed, bpODN and ODN differently affected the intracellular calcium dynamics. ODN increased calcium event frequency at the lowest concentration used (10^{-10} M), and its stimulating effect gradually decreased for higher concentrations (10^{-9} and 10^{-8} M) until a value lower than the control one for 10^{-7} M. At 10^{-7} M, ODN also modified the average shape of each single event by reducing their amplitude and rising time, and by increasing their duration in comparison to control conditions. In accordance to these observations, it has been previously reported that ODN increases $[Ca^{2+}]_i$ in silent rat astrocytes and that micromolar ODN concentrations elicit weaker increases in $[Ca^{2+}]_i$ than nanomolar concentrations (Gandolfo et al., 1997; Leprince et al., 1998). Interestingly, bpODN produced a perfect mirror image to the ODN effect. Since it has previously been demonstrated that ODN activated the metabotropic receptor for nanomolar concentrations (Gandolfo et al., 1997; Leprince et al., 1998) and CBR for micromolar concentrations (De Mateos-Verchère et al., 1998) we could speculate that the dose-dependent effect of ODN on calcium event frequency is representative of a receptor selectivity switch from the ODN-GPCR to the CBR. Conversely, bpODN would target CBR for weak concentration and the ODN-GPCR for higher concentration.

In vivo effects of bpODN and ODN were evaluated in two paradigms involving either the metabotropic receptor

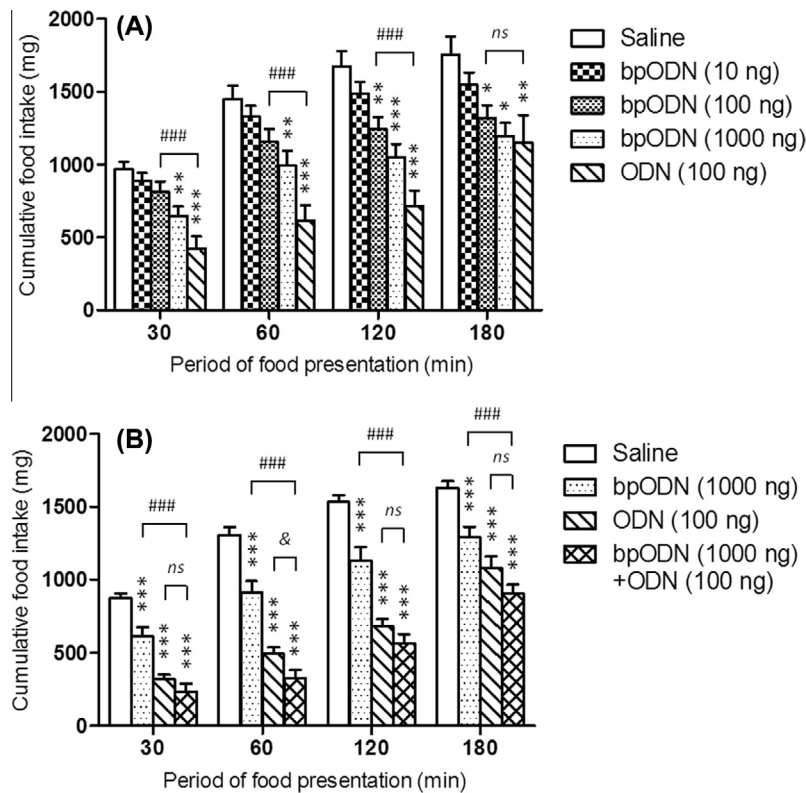


Fig. 7. Time course of the effect of bpODN, ODN and bpODN + ODN on food intake in food-deprived mice. (A) Mice deprived of food for 18 h were injected icv (10 μ l) with saline, bpODN (10, 100 or 1000 ng/mouse), or ODN (100 ng/mouse). Ten min after icv injection, each animal had access to a weighed food pellet (5 g) and its cumulative consumption was measured at defined time points over a 3-h period. Data represent mean \pm SEM of 12 mice per group. Statistical significance was assessed using a one-way ANOVA and a post hoc multiple comparison Student–Newman–Keuls test. * p < 0.05, ** p < 0.01, *** p < 0.001 vs saline-injected mice, ### p < 0.001, ns not significantly different for bpODN vs ODN. (B) Mice deprived of food for 18 h were injected icv (10 μ l) with saline, bpODN (1000-ng/mouse), ODN (100-ng/mouse) or bpODN + ODN (1000-ng + 100-ng/mouse, respectively). Ten min after icv injection, each animal had access to a weighed food pellet (5 g) and its cumulative consumption was measured at defined time points over a 3-h period. Data represent mean \pm SEM of 12 mice per group. Statistical significance was assessed using a one-way ANOVA and a post hoc multiple comparison Student–Newman–Keuls test. *** p < 0.001 vs saline-injected mice, ### p < 0.001 for bpODN + ODN vs bpODN, & p < 0.05, ns not significantly different for bpODN + ODN vs ODN.

Table 3. Effects of bpODN and ODN on elevated zero-maze test in mice

Treatment	Total distance traveled (cm)	Number of entries into open quadrants	Percent of time spent into open quadrants
Saline, 10 μ l	2796 \pm 204	65.0 \pm 4.1	50.63 \pm 3.15
bpODN, 10 ng/10 μ l	2817 \pm 201	61.9 \pm 4.4 ^{ns}	46.59 \pm 2.63 ^{ns}
bpODN, 100 ng/10 μ l	2048 \pm 236	50.4 \pm 3.2*	38.56 \pm 3.06*
bpODN, 1000 ng/10 μ l	1925 \pm 267*	41.7 \pm 4.2**	31.94 \pm 4.35**
ODN, 100 ng/10 μ l	2120 \pm 154	39.4 \pm 4.9***	27.72 \pm 3.88***

Mice were injected icv with saline, bpODN, or ODN, and 90 min later, they were placed at the end of the open section. Data represent mean \pm SEM of 12 mice per group. Statistical significance was assessed using a one-way ANOVA and a post hoc multiple comparison Student–Newman–Keuls test.

* p < 0.05.

** p < 0.01.

*** p < 0.001.

^{ns} not significantly different vs saline-injected mice.

or the CBR. It has been previously shown that icv administration of nanomolar doses of ODN significantly reduced food intake in fasted mice and that this effect is mediated by the metabotropic receptor (De Mateos-Verchère et al., 2001; Do Rego et al., 2007). We showed that bpODN mimicked the anorexigenic effect of ODN, although its efficacy and potency were weaker. The comparable inhibition of food consumption was achieved with approximately a ten-fold higher dose of bpODN than

ODN. Moreover, co-administration of bpODN and ODN did not provoke a synergistic effect on food intake. Consistent to the data obtained *in vitro*, this weak anorexigenic effect of bpODN can likely be ascribed to its lower affinity to the metabotropic receptor.

The GABA_A receptors are composed of five protein subunits that form a central chloride selective ion channel. The majority of GABA_A receptors is composed of α , β , and γ subunits and contain the classical binding

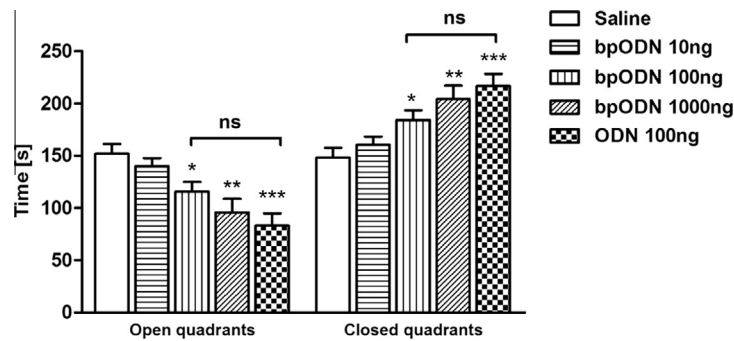


Fig. 8. Effect of bpODN and ODN on time spent in open and closed quadrants of elevated zero-maze. Mice were injected icv with saline, bpODN (10, 100, 1000 ng/mouse) or ODN (100 ng/mouse) and 90 min later animals were placed at the end of the open section for a 5-min period. Data represent mean \pm SEM of 12 mice per group. Statistical significance was assessed using a one-way ANOVA and a post hoc multiple comparison Student–Newman–Keuls test. * $p < 0.05$, ** $p < 0.01$, *** $p < 0.001$ vs saline-injected mice, ns not significantly different for bpODN vs ODN.

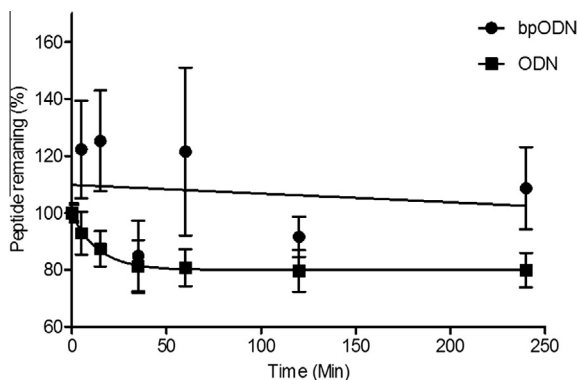


Fig. 9. Degradation kinetics of ODN (■) and bpODN (●) evaluated by UPLC-mass spectrometry analysis after incubation of the peptide in rat CSF. Each point is the mean \pm SEM of three independent experiments.

pocket for benzodiazepines, located in a subunit cleft between $\alpha 1,2,3,5$ and $\gamma 2$ subunits (Sieghart and Sperk, 2002; Sigel et al., 2006). More recently, a new modulator site for benzodiazepines at the $\alpha 1/\beta 2$ subunit interface, homologous to the classical benzodiazepine binding pocket, has been also postulated (Sigel and Lüscher, 2011). Depending on the receptor subunit composition or modulator site used, endozepines can act as positive or negative allosteric modulators of GABA_A receptors (D’Hulst et al., 2009). As a negative allosteric modulator of the CBR, ODN blocks GABA-induced Cl[−] efflux in the GABA_A receptors and reduces the inhibitory post-synaptic potentials by inhibiting GABA-induced currents (Bormann, 1991; Louiset et al., 1993; Alfonso et al., 2012). More recently, a role of positive allosteric modulator of CBR has been demonstrated (Christian et al., 2013). Thus, secretion of ODN by glial cells could provide an important mechanism by which inhibition is modulated in the CNS. Qian et al. (2008), reported that phosphorylation of ODN may be required for optimal binding to GABA_A receptors (Qian et al., 2008). They show, using a competition assay, that bpODN has a stronger affinity for the GABA_A $\alpha 1$ subunit, isolated from the rabbit cerebellum, than unphosphorylated ODN or DBI. Thus, the anxiogenic property of ODN was used as a test for the selectivity toward

CBRs. Interestingly, we showed that the anxiogenic effect of bpODN was weaker than the effect exerted by ODN, suggesting that bpODN interacts with CBR with a lower affinity. An explanation for this discrepancy with Qian et al. could lie in the GABA_A receptor subunit composition that may differ between the cerebellum and other structures involved in the anxiogenic effect. Indeed, ODN binds the α subunit of the GABA_A receptor complex (Qian et al., 2008) to exert its anxiogenic effect. The weakest anxiogenic potency of bpODN could be related to an altered interaction with the GABA_A α subunit or with another subunit.

CONCLUSION

In the present study, we have shown that cortical astrocytes, like Müller glial cells release bpODN and also two other active peptides, [μ Glu¹]ODN and OP. Our results showed that phosphorylation of ODN resulted in a remarkable decrease in metabotropic receptor functionality and did not support that this post-translational modification is involved in receptor selectivity. The weak effect on GABA_A receptor may be associated with its lower receptor affinity or may be related to its interaction with other GABA_A receptor subunits. Further experiments allowing to precisely quantify the endozepine molecular forms in the cultured astrocyte supernatants as well as the developments of models containing different GABA_A receptor subtypes may provide an interesting approach for further understanding the biological relevance of bpODN action.

Acknowledgments—This work was supported by grants from Inserm, European Regional Development Fund (ERDF) PeReNE, and Polish Ministry of Science ‘Mobilnosc Plus 625/MOB/743/2011/0’ (K.G.).

REFERENCES

- Alfonso J, Le Magueresse C, Zuccotti A, Khodosevich K, Monyer H (2012) Diazepam binding inhibitor promotes progenitor proliferation in the postnatal SVZ by reducing GABA signaling. *Cell Stem Cell* 10:76–87.
- Barmack NH, Bilderback TR, Liu H, Qian Z, Yakhnitsa V (2004) Activity-dependent expression of acyl-coenzyme A-binding

- protein in retinal Müller glial cells evoked by optokinetic stimulation. *J Neurosci* 24:1023–1033.
- Bormann J (1991) Electrophysiological characterization of diazepam binding inhibitor (DBI) on GABA_A receptors. *Neuropharmacology* 30:1387–1389.
- Christian CA, Herbert AG, Holt RL, Peng K, Sherwood KD, Pangratz-Fuehrer S, Rudolph U, Huguenard JR (2013) Endogenous positive allosteric modulation of GABA(A) receptors by diazepam binding inhibitor. *Neuron* 78:1063–1074.
- Compère V, Li S, Leprince J, Tonon MC, Vaudry H, Pelletier G (2003) Effect of intracerebroventricular administration of the octadecaneuropeptide on the expression of pro-opiomelanocortin, neuropeptide Y and corticotropin-releasing hormone mRNAs in rat hypothalamus. *J Neuroendocrinol* 15:197–203.
- Compère V, Li S, Leprince J, Tonon MC, Vaudry H, Pelletier G (2004) *In vivo* action of a new octadecaneuropeptide (ODN) antagonist on gonadotropin-releasing hormone gene expression in the male rat brain. *Neuroscience* 125:411–415.
- Compère V, Li S, Leprince J, Tonon MC, Vaudry H, Pelletier G (2005) *In vivo* action of a new octadecaneuropeptide antagonist on neuropeptide Y and corticotropin-releasing hormone mRNA levels in rat. *Mol Brain Res* 141:156–160.
- De Bock M, Decrock E, Wang N, Bol M, Vinken M, Bultynck G, Leybaert L (2014) The dual face of connexin-based astroglial Ca²⁺ communication: a key player in brain physiology and a prime target in pathology. *Biochim Biophys Acta* 1843:2211–2232.
- De Mateos-Verchère JG, Leprince J, Tonon MC, Vaudry H, Costentin J (1998) The octadecaneuropeptide ODN induces anxiety in rodents: possible involvement of a shorter biologically active fragment. *Peptides* 19:841–848.
- De Mateos-Verchère J, Leprince J, Tonon MC, Vaudry H, Costentin J (1999) Reduction of pentylenetetrazol-induced convulsions by the octadecaneuropeptide ODN. *Peptides* 20:1431–1436.
- De Mateos-Verchère JG, Leprince J, Tonon MC, Vaudry H, Costentin J (2001) The octadecaneuropeptide [diazepam-binding inhibitor (33–50)] exerts potent anorexigenic effects in rodents. *Eur J Pharmacol* 414:225–231.
- D'Hulst C, Atack JR, Kooy RF (2009) The complexity of the GABA_A receptor shapes unique pharmacological profiles. *Drug Discov Today* 14:866–875.
- Do Rego JL, Mensah-Nyagan AG, Beaujean D, Leprince J, Tonon MC, Luu-The V, Pelletier G, Vaudry H (2001) The octadecaneuropeptide ODN stimulates neurosteroid biosynthesis through activation of central-type benzodiazepine receptors. *J Neurochem* 76:128–138.
- Do Rego JC, Orta MH, Leprince J, Tonon MC, Vaudry H, Costentin J (2007) Pharmacological characterization of the receptor mediating the anorexigenic action of the octadecaneuropeptide: evidence for an endozepine tone regulating food intake. *Neuropsychopharmacology* 32:1641–1648.
- Dong E, Matsumoto K, Tohda M, Watanabe H (1999) Involvement of diazepam binding inhibitor and its fragment octadecaneuropeptide in social isolation stress-induced decrease in pentobarbital sleep in mice. *Life Sci* 64:1779–1784.
- Ferrero P, Guidotti A, Conti-Tronconi B, Costa E (1984) A brain octadecaneuropeptide generated by tryptic digestion of DBI (diazepam binding inhibitor) functions as a proconflict ligand of benzodiazepine recognition sites. *Neuropharmacology* 23:1359–1362.
- Ferrero P, Santi MR, Conti-Tronconi B, Costa E, Guidotti A (1986) Study of an octadecaneuropeptide derived from diazepam binding inhibitor (DBI): biological activity and presence in rat brain. *Proc Natl Acad Sci USA* 83:827–831.
- Gandolfo P, Patte C, Leprince J, Thoumas JL, Vaudry H, Tonon MC (1997) The stimulatory effect of the octadecaneuropeptide (ODN) on cytosolic calcium in rat astrocytes is not mediated through classical benzodiazepine receptors. *Eur J Pharmacol* 322:275–281.
- Gandolfo P, Patte C, Thoumas JL, Leprince J, Vaudry H, Tonon MC (1999) The endozepine ODN stimulates [³H]thymidine incorporation in cultured rat astrocytes. *Neuropharmacology* 38:725–732.
- Graves JD, Krebs EG (1999) Protein phosphorylation and signal transduction. *Pharmacol Ther* 82:111–121.
- Guidotti A, Forchetti CM, Corda MG, Kondel D, Bennett CD, Costa E (1983) Isolation, characterization and purification to homogeneity of an endogenous polypeptide with agonistic action on benzodiazepine receptors. *Proc Natl Acad Sci USA* 80:3531–3535.
- Haley TJ, McCormick WG (1957) Pharmacological effects produced by intracerebral injection of drugs in the conscious mouse. *Br J Pharmacol Chemother* 12:12–15.
- Hamdi Y, Masmoudi-Kouki O, Kaddour H, Belhadj F, Gandolfo P, Vaudry D, Mokni M, Leprince J, Hachem R, Vaudry H, Tonon MC, Amri M (2011) Protective effect of the octadecaneuropeptide on hydrogen peroxide-induced oxidative stress and cell death in cultured rat astrocytes. *J Neurochem* 118:416–428.
- Hamdi Y, Kaddour H, Vaudry D, Bahdoudi S, Douiri S, Leprince J, Castel H, Vaudry H, Tonon MC, Amri M, Masmoudi-Kouki O (2012) The octadecaneuropeptide ODN protects astrocytes against hydrogen peroxide-induced apoptosis via a PKA/MAPK-dependent mechanism. *PLoS One* 7:e42498.
- Hoffmann R, Metzger S, Spengler B, Otvos Jr L (1999) Sequencing of peptides phosphorylated on serines and threonines by post-source decay in matrix-assisted laser desorption/ionization time-of-flight mass spectrometry. *J Mass Spectrom* 11:1195–1204.
- Holländer H, Makarov F, Dreher Z, van Driel D, Chan-Ling TL, Stone J (1991) Structure of the macroglia of the retina: sharing and division of labour between astrocytes and Muller cells. *J Comp Neurol* 313:587–603.
- Hubbard MJ, Cohen P (1993) On target with a new mechanism for the regulation of protein phosphorylation. *Trends Biochem Sci* 18:172–177.
- Kastin AJ, Banks WA, Hahn K, Zadina JE (1994) Extreme stability of Tyr-MIF-1 in CSF. *Neurosci Lett* 174:26–28.
- Kavaliers M, Hirst M (1986) An octadecaneuropeptide (ODN) derived from diazepam binding inhibitor increases aggressive interactions in mice. *Brain Res* 383:343–349.
- Lamacz M, Tonon MC, Smih-Rouet F, Patte C, Gasque P, Fontaine M, Vaudry H (1996) The endogenous benzodiazepine receptor ligand ODN increases cytosolic calcium in cultured rat astrocytes. *Brain Res Mol Brain Res* 37:290–296.
- Lanfray D, Arthaud S, Ouellet J, Compère V, Do-Régo JL, Leprince J, Lefranc B, Castel H, Bouchard C, Monge-Roffarello B, Richard D, Pelletier G, Vaudry H, Tonon MC, Morin F (2013) Gliotransmission and brain glucose sensing. Critical role of endozepines. *Diabetes* 62:801–810.
- Leprince J, Gandolfo P, Thoumas JL, Patte C, Fauchère JL, Vaudry H, Tonon MC (1998) Structure-activity relationships of a series of analogues of the octadecaneuropeptide ODN on calcium mobilization in rat astrocytes. *J Med Chem* 41:4433–4438.
- Leprince J, Oulyadi H, Vaudry D, Masmoudi O, Gandolfo P, Patte C, Costentin J, Fauchère JL, Davoust D, Vaudry H, Tonon MC (2001) Synthesis, conformational analysis and biological activity of cyclic analogs of the octadecaneuropeptide ODN. Design of a potent endozepine antagonist. *Eur J Biochem* 268:6045–6057.
- Louiset E, Vaudry H, Cazin L (1993) Allosteric modulation of the GABA-induced chloride current in frog melanotrophs. *Ann N Y Acad Sci* 680:564–566.
- Malagon M, Vaudry H, Van Strien F, Pelletier G, Gracia-Navarro F, Tonon MC (1993) Ontogeny of diazepam-binding inhibitor related peptides (endozepines) in the rat brain. *Neuroscience* 57:777–786.
- Manabe Y, Toyoda T, Kuroda K, Imaizumi M, Yamamoto T, Fushiki T (2001) Effect of diazepam binding inhibitor (DBI) on the fluid intake, preference and the taste reactivity in mice. *Behav Brain Res* 126:197–204.
- Masmoudi O, Gandolfo P, Tokay T, Leprince J, Ravni A, Vaudry H, Tonon MC (2005) Somatostatin down-regulates the expression and release of endozepines from cultured rat astrocytes via distinct receptor subtypes. *J Neurochem* 94:561–571.

- Neveu C, Lefranc B, Tasseau O, Do Régo JC, Bourmaud A, Chan P, Bauchat P, Le Marec O, Chuquet J, Guilhaudis L, Boutin JA, Ségalas-Milazzo I, Costentin J, Vaudry H, Baudy-Floc'h M, Vaudry D, Leprince J (2012) Rational design of a low molecular weight, stable, potent and long-lasting GPR103 aza- β 3 pseudopeptide agonist. *J Med Chem* 55:7516–7524.
- Parri HR, Crunelli V (2003) The role of Ca^{2+} in the generation of spontaneous astrocytic Ca^{2+} oscillations. *Neuroscience* 120:979–992.
- Patte C, Vaudry H, Desrues L, Gandolfo P, Strijdsveen I, Lamacz M, Tonon MC (1995) The endozepine ODN stimulates polyphosphoinositide metabolism in rat astrocytes. *FEBS Lett* 362:106–110.
- Pawson T, Scott JD (1997) Signaling through scaffold, anchoring, and adaptor proteins. *Science* 278:2075–2080.
- Qian Z, Bilderback TR, Barmack NH (2008) Acyl coenzyme A-binding protein (ACBP) is phosphorylated and secreted by retinal Müller astrocytes following protein kinase C activation. *J Neurochem* 105:1287–1299.
- Schipke CG, Heidemann A, Skupin A, Peters O, Falcke M, Kettenmann H (2008) Temperature and nitric oxide control spontaneous calcium transients in astrocytes. *Cell Calcium* 43:285–295.
- Servili A, Le Page Y, Leprince J, Caraty A, Escobar S, Parhar IS, Seong JY, Vaudry H, Kah O (2011) Organization of two independent kisspeptin systems derived from evolutionary-ancient kiss genes in the brain of zebrafish. *Endocrinology* 152:1527–1240.
- Shumyantseva VV, Suprun EV, Bulko TV, Archakov AI (2014) Electrochemical methods for detection of post-translational modifications of proteins. *Biosens Bioelectron* 61:131–139.
- Sieghart W, Sperk G (2002) Subunit composition, distribution and function of GABA(A) receptor subtypes. *Curr Top Med Chem* 2:795–816.
- Sigel E, Lüscher BP (2011) A closer look at the high affinity benzodiazepine binding site on GABA_A receptors. *Curr Top Med Chem* 11:241–246.
- Sigel E, Baur R, Boulineau N, Minier F (2006) Impact of subunit positioning on GABA_A receptor function. *Biochem Soc Trans* 34:868–871.
- Slobodyansky E, Guidotti A, Wambebe C, Berkovich A, Costa E (1989) Isolation and characterization of a rat brain triakontatetrapeptide, a posttranslational product of diazepam binding inhibitor: specific action at the Ro 5-4864 recognition site. *J Neurochem* 53:1276–1284.
- Tonon MC, Désy L, Nicolas P, Vaudry H, Pelletier G (1990) Immunocytochemical localization of the endogenous benzodiazepine ligand octadecaneuropeptide (ODN) in the rat brain. *Neuropeptides* 15:17–24.
- Tonon MC, Leprince J, Morin F, Gandolfo P, Compère V, Pelletier G, Malagon MM, Vaudry H (2013) Endozepines. In: Kastin AJ, editor. *Handbook of biologically active peptides*. New York: Elsevier. p. 760–765.
- Vaudry H, Tonon MC, Delarue C, Vaillant R, Kraicer J (1978) Biological and radioimmunological evidence for melanocyte stimulating hormones (MSH) of extrapituitary origin in the rat brain. *Neuroendocrinology* 27:9–24.
- Vidnyánszky Z, Görcs TJ, Hámori J (1994) Diazepam binding inhibitor fragment 33–50 (octadecaneuropeptide) immunoreactivity in the cerebellar cortex is restricted to glial cells. *Glia* 10:132–141.
- Yanase H, Shimizu H, Yamada K, Iwanaga T (2002) Cellular localization of the diazepam binding inhibitor in glia cells with special reference to its coexistence with brain-type fatty acid binding protein. *Arch Histol Cytol* 65:27–36.

(Accepted 5 January 2015)
(Available online 30 January 2015)